Thin Solid Films 518 (2010) 5525–5529

Contents lists available at ScienceDirect

Thin Solid Films

journal homepage: www.elsevier.com/locate/tsf

Femtosecond laser deposition of TiO_2 by laser induced forward transfer

M. Sanz [a,*], M. Walczak [a], M. Oujja [a], C. Domingo [b], A. Klini [c], E.L. Papadopoulou [c], C. Fotakis [c], M. Castillejo [a]

[a] Instituto de Química Física Rocasolano, CSIC, Serrano 119, 28006 Madrid, Spain
[b] Instituto de Estructura de la Materia, CSIC, Serrano 123, 28006 Madrid, Spain
[c] Institute of Electronic Structure and Lasers, Foundation for Research and Technology-Hellas, P.O. Box 1385, 71110 Heraklion, Greece

ARTICLE INFO

Article history:
Received 29 July 2009
Received in revised form 15 March 2010
Accepted 22 April 2010
Available online 29 April 2010

Keywords:
TiO_2
Laser deposition
Laser induced forward transfer
Nanostructures
Titanium dioxide
Scanning electron microscopy
X-ray diffraction
Raman spectroscopy

ABSTRACT

Femtosecond lasers have been used for laser induced forward transfer (LIFT) of TiO_2, a wide-band semiconductor with many industrial and research applications. TiO_2 polycrystalline thin films on quartz (obtained by pulsed laser deposition) were used as donors and both quartz and fluorine-doped tin dioxide coated glass substrates as acceptors. LIFT was performed at the laser wavelengths of 248 and 800 nm with pulses of 450 and 300 fs respectively. The transferred material was characterized by energy-dispersive X-ray spectroscopy, X-ray diffraction and micro-Raman spectroscopy to determine the composition and crystalline quality, and by scanning electron microscopy and atomic force microscopy to assess the surface morphology. The relation between these properties and the laser transfer conditions, including wavelength, pulse energy and acceptor substrate, are presented.

1. Introduction

Laser induced forward transfer (LIFT) is a deposition method in which a pulsed laser beam is focused through a transparent support onto a thin film of the material to be transferred [1–3]. Under laser irradiation, a micrometer sized droplet of film material is ejected and transported onto a receptor surface placed nearby. This method allows the fabrication of a customer defined pattern with a high lateral resolution onto any substrate of a broad range of materials, such as oxides [3–14], metals [1,2,15–18], conducting polymers [19] and biomaterials [20,21].

In LIFT, the use of nanosecond (ns) laser pulses presents some difficulties associated with heating effects, such as remelting of the transferred material by the trailing part of the laser pulse [4], non precise material processing and the spatial limitations of the transferred material by the laser focal spot size. The use of femtosecond (fs) pulses overcomes some of these difficulties and enables deposition of microsized features with high spatial resolution, good control over the morphology and composition and noticeable reduction of the characteristic dimensions [4–7,17–19]. Another important feature of fs pulses is that the LIFT threshold fluence is reduced compared to that of ns pulses [15], which constitutes an advantage for deposition of transparent materials. With LIFT, arrays of spots with size down to 300 nm can be obtained [17] using laser wavelengths corresponding to the absorption band of the donor material. Temporal shaping has been proposed as a tool to further control the morphology of structures obtained by this technique [18].

In some studies [10–12,19–22] a sacrificial material layer is inserted between the carrier substrate and the layer of the material to be transferred and the influence of its thickness has been determined [22]. The purpose of the sacrificial layer is to absorb part of the laser pulse energy and ensure a gentle transferring process. However, in some cases it has been observed that the sacrificial layer may cause some debris that pollutes the LIFT material [21,22].

TiO_2 is an *n*-type, wide-band semiconductor, with many industrial and research applications [23–25]. The two crystalline phases of TiO_2 are rutile and anatase, with energy bandgap 3.0 and 3.2 eV, respectively. The dependence of properties on its nanostructure [26] has motivated the use of nanometer-sized TiO_2 particles for ceramics, optical devices, sensors, self cleaning coatings, fabrication of electrodes for photovoltaics, etc. Using a mixture of TiO_2 and gold as donor, LIFT deposits have been obtained with ns laser pulses at 532 nm [10]. Doping with gold changes the bandgap allowing tuning it to the laser photon energy and ensuring an efficient laser material interaction. In another study [8], the influence of a sacrificial layer of gold for LIFT of TiO_2 has been investigated. The velocity of the droplets during the transfer process was found to depend on the sacrificial layer thickness.

Aiming at the understanding of the different mechanisms involved in the process and their dependence on the irradiation wavelength, in this work we present results on the growth of TiO_2 deposits by fs LIFT.

* Corresponding author.
E-mail address: mikel.sanz@iqfr.csic.es (M. Sanz).

0040-6090/$ – see front matter © 2010 Elsevier B.V. All rights reserved.
doi:10.1016/j.tsf.2010.04.057

This study also aims at exploring the possibility of controlling the structure of the transferred material by choosing the adequate laser parameters. We have selected quartz and fluorine-doped tin dioxide (FTO) coated glass as LIFT substrates. The selection of the latter is justified by its use in dye sensitized solar cells (DSSC) for photovoltaics [25]. In fact, this material has been used as LIFT substrate of anatase phase TiO_2 in this type of applications [13,14]. In particular, it has been recently proven that the performance of the rutile phase of TiO_2 is comparable to the anatase phase, with additional advantages of the former, including better chemical stability and higher refractive index [27 and references therein]. As donors we use TiO_2 films fabricated by pulsed laser deposition (PLD). LIFT was operated at two wavelengths (248 and 800 nm), which correspond to photon energies respectively above and below the bandgap of the starting rutile material. The laser pulses had durations of 450 and 300 fs respectively. The morphology of the transferred patterns was characterized by scanning electron microscopy (SEM) and atomic force microscopy (AFM). The composition of deposits was investigated through energy-dispersive X-ray spectroscopy (EDX) and the crystallinity of the prepared donors and of the deposits was measured by X-ray diffraction (XRD) and micro-Raman spectroscopy.

2. Experimental details

The donor was a 1 mm thick quartz window covered by a 70 nm nanostructured layer of TiO_2 prepared by PLD, using TiO_2 rutile sintered pellets and a KrF excimer laser (Lambda Physik, 248 nm, pulse duration 34 ns, 10 Hz) operating at a fluence of 2 J/cm^2. Deposition was carried out under 0.5 Pa of oxygen while the quartz substrates were placed parallel to the target at a distance of 4 cm and heated up to 650 °C [28].

Quartz or FTO coated glass pieces were used as acceptor for LIFT. Prior to use, the substrates were ultrasonically degreased in acetone and isopropanol for 10 min. Two experimental setups with two different subpicosecond laser systems operating at 248 and 800 nm were employed. Detailed descriptions are given in [4] and [18] respectively. The two laser sources are: a) a hybrid distributed feedback dye laser/KrF excimer laser with top hat beam profile (248 nm, 4 Hz, pulse duration of 450 fs) and b) an amplified Ti: Sapphire laser with Gaussian beam profile (800 nm, 1 Hz, pulse duration of 300 fs).

The donor–acceptor pair, placed in contact, was positioned in a computer controlled *x*–*y* translation stage, allowing a maximum movement of 25×25 mm^2 with resolution of 1.25 μm in any user defined pattern. The prepared samples, covering an area of 2×2 mm^2, consist in a square array of 34×34 spots with centres separated by a distance of 60 μm. The laser beam was focused onto the donor surface through microscope objectives 25× and 20×, for 248 and 800 nm, respectively. The size of the focal spots is 25×20 μm^2 and 10 μm diameter, respectively. During the transfer the donor area was viewed through a CCD camera. All the LIFT experiments were performed under ambient pressure and temperature conditions. The composition and crystallinity of deposits were investigated through energy-dispersive X-ray spectroscopy (EDX), X-ray diffraction (XRD) and micro-Raman spectroscopy. The EDX system used is an Isis Link (Oxford) integrated in a scanning electron microscopy (SEM, Zeiss DSM-960) and was operated at 15 kV. The XRD apparatus was a Bruker AXS D8 Advance powder diffractometer with Cu Kα radiation at $\theta/2\theta$ configuration. Micro-Raman spectra were obtained with a Renishaw Raman Microscope System RM2000 equipped with a Leica microscope, using magnification 50×, an electrically refrigerated CCD camera and an Ar laser at 514 nm operating at a power level of 3 mW as excitation source. The spectra were taken with a spectral resolution of 4 cm^{-1} and exposure times in the range of 10–60 s. The morphology of the LIFT deposits was examined by SEM (Philips XL30). Observation by SEM of quartz and FTO coated glass substrates revealed a flat surface in the former and a rough nanostructured surface with typical sizes from 50 to 200 nm in the latter. Sample thickness was measured by AFM (Veeco Nanoscope IIIa).

3. Results and discussion

The donor substrates, consisting on a quartz window covered by a 70 nm thick layer of TiO_2 prepared by PLD, were analyzed by XRD. As shown in Fig. 1, the material was found to be polycrystalline TiO_2 containing a rutile phase with (100) and (200) orientations. The micro-Raman spectra acquired on the donor substrates confirm the presence of the rutile phase [29].

LIFT patterns were fabricated at 248 nm with two different pulse energies of 2 and 22 nJ per pulse, where the highest energy was chosen to be below the substrate damage threshold. EDX analyses confirm the presence of titanium in the transferred material. The crystallinity of the transfers was characterized by micro-Raman spectroscopy (Fig. 2). In this figure the spectrum of the printed material is compared with the spectra of the quartz and FTO substrates and with that of a pressed pure rutile disk. It is observed that the spectra contain features at 240, 448 and 610 cm^{-1}, assigned to the rutile phase [29]. On the quartz substrate (Fig. 2a), the use of low laser pulse energy (2 nJ) ensures the crystallinity of the transferred material, while at higher energy (22 nJ) the deposits are either amorphous or the peaks indicative of crystallinity are below the detection limit.

By using FTO coated glass as substrate (Fig. 2b), the TiO_2 printed material is crystalline in all the explored energy range, as evidenced by the presence of the rutile peaks in the micro-Raman spectra. At low energy (2 nJ), the intensity of the rutile peaks is 5 times higher than at 22 nJ, indicating a higher amount of crystalline material at low energy. The different degree of crystallinity of the deposits obtained at high pulse energies on the two types of substrate can be related with the differences in their morphology; in fact, as mentioned, the FTO based substrates present a rough surface at the nanometer scale that can act as a field of nucleation centres for crystalline rutile TiO_2 [30]. Also, the lattice mismatch between the material to be deposited and the substrate has been discussed as an important factor influencing the nucleation and growth of deposits [27,31]. In our case the small lattice mismatch between FTO and rutile TiO_2 [27] plays a key role for deposition of rutile TiO_2 crystalline nanoparticles on this substrate.

At low energy (2 nJ), the spots transferred at 248 nm on quartz, as observed by SEM (Fig. 3a), consist of well delimited rectangles (of around 30×25 μm^2), indicating that transfer is mediated by melt-through of the donor film [17], where the printed material reflects the shape of the laser spot. At high energy (22 nJ), the transferred rectangular spots are somewhat larger and microparticulates are

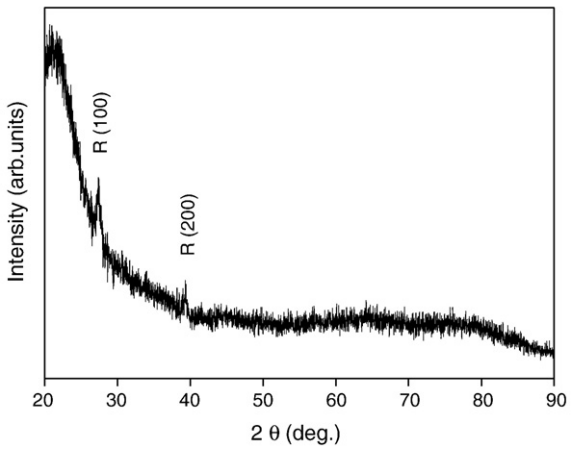

Fig. 1. XRD pattern of donor TiO_2 material. R refers to rutile phase.

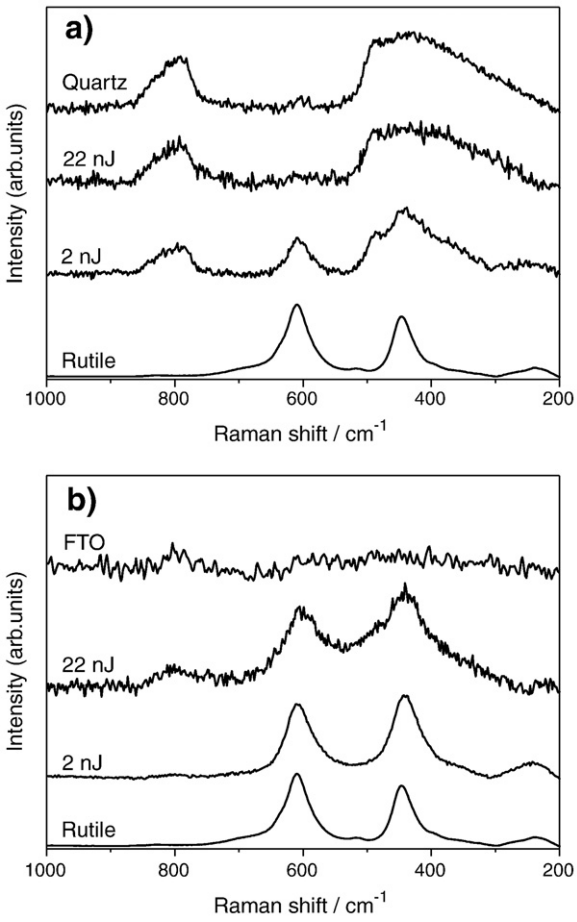

Fig. 2. Micro-Raman spectra of TiO_2 deposited on a) quartz and b) FTO by LIFT at 2 nJ and 22 nJ, as indicated. For comparison spectra of pure rutile TiO_2 and quartz and FTO substrates are shown.

observed in the surroundings (Fig. 3b). A similar dependence of size and structure of the printed material has been reported for Cr [5,17], Pt and In_2O_3 [5] and Zn and ZnO [7]. This phenomenon of coalescence has been related with spallation processes, where the extent of splashing and the print size is influenced and can be controlled by the laser fluence.

A higher magnification image taken inside of a printed TiO_2 feature (Fig. 3c) shows an underlying irregular layer, about 20 nm thick as measured by AFM, covered by grains with widely spread sizes, ranging from 20 to 200 nm. Similar morphologies have been observed in the LIFT printing of Zn [7,17]; in this case nanoparticles with nano and micrometer sizes were observed instead of a continuous deposited film. The higher amount of delocalized microparticles observed at high pulse energy in LIFT of TiO_2 is related with the higher contribution of the process of spallation during LIFT [32]. In fact, at energies above the LIFT threshold, the removed material constitutes an energetic plasma of electrons, ions, atoms, molecules and fragments. The high temperature of the ejected material prevents deposition in the central part of the spot, whereas condensation takes place in the cooler edges [5].

Transference to FTO coated glass substrates (Fig. 4) shows similar behaviour to that described previously for quartz although EDX analysis indicates a somewhat larger amount of titanium. At low pulse energy (2 nJ), the material is spatially concentrated in rectangles with uniform size of $25 \times 20\ \mu m^2$ (Fig. 4a). A closer look inside the spots reveals a large amount of irregular shaped material with many overimposed particulates, ranging in size from 40 to 350 nm (Fig. 4b). At high energy (22 nJ), the transference of material is more

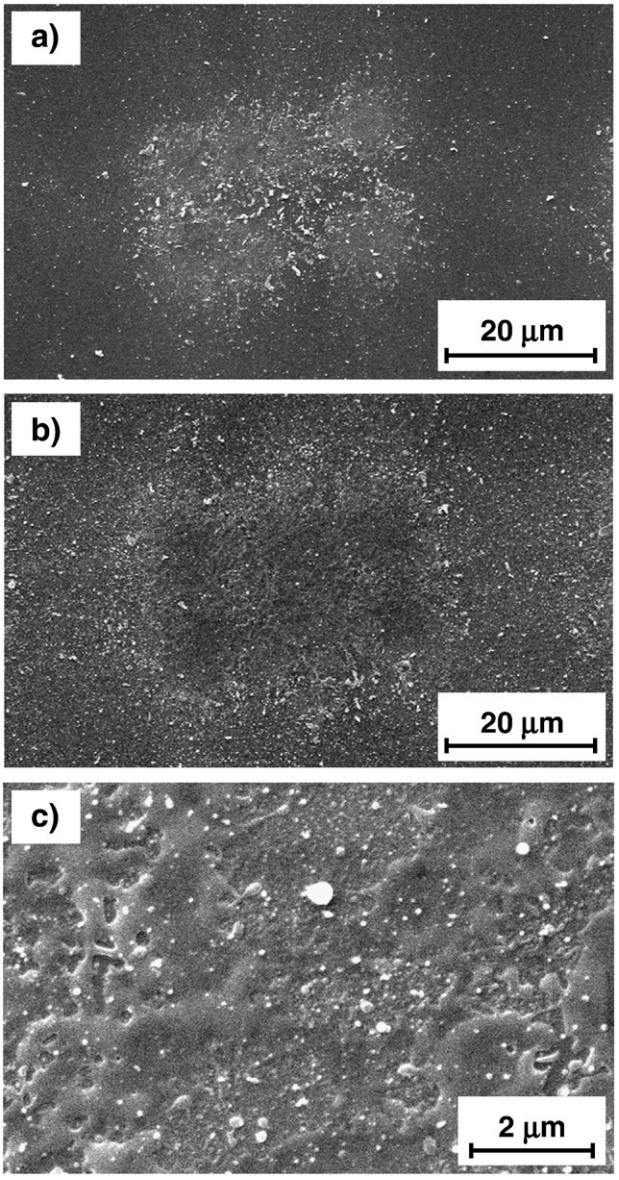

Fig. 3. SEM images of laser induced forward transferred TiO_2 at 248 nm on quartz at: a) 2 nJ and b) 22 nJ; image c) shows an enlarged view of LIFT material in a).

delocalized. It is also observed that the size and density of the transferred particulates scale with pulse energy, presenting a similar morphology to that observed for quartz, but with larger nanoparticles and wider size spread. Also the thickness of material deposited on FTO, about 35 nm, is larger than on quartz.

Thus, regarding the two types of substrates used, the main difference observed at 248 nm is that on quartz the crystallinity of the deposits depends on the laser pulse energy, while on FTO at all pulse energies the printed material is crystalline. Regarding the surface morphology, deposits on quartz are more uniform with particulates of 20–200 nm diameter, whereas in the case of FTO the density and size of particulates are higher, with diameters in the range of 40–350 nm.

Experiments were also performed at 800 nm using an energy per pulse of 84 nJ, which is the minimum required to observe transfer to the acceptor substrate. The printed material covers the substrate in a rather delocalized area. Again at this wavelength EDX measurements indicate a titanium based deposit with similar abundance irrespective of the substrate used. The titanium EDX signals of deposits grown at 800 nm are less intense than those grown at 248 nm, a fact that is

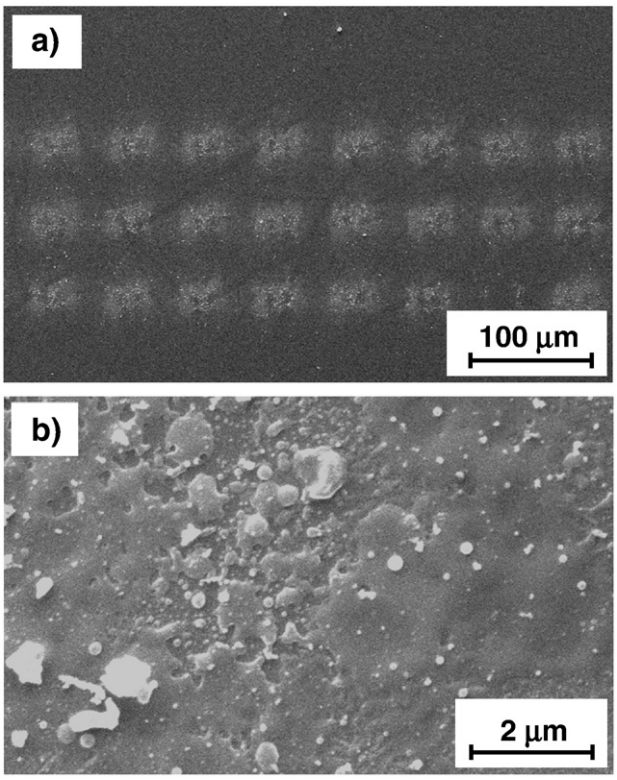

Fig. 4. SEM images of laser induced forward transferred TiO_2 at 248 nm FTO coated glass at 2 nJ: a) array of spots and b) shows an enlarged view of LIFT material in a).

related to the reduced thickness of the transfers. As measured by micro-Raman spectroscopy (not shown), the material is not crystalline when deposited on quartz. However on FTO, a small peak around 450 cm^{-1} indicates the presence of the crystalline rutile phase. As previously mentioned for LIFT at 248 nm, the different crystallinity of the material printed at 800 nm on the two different substrates is assigned to differences in their superficial morphology. Fig. 5 shows a mostly delocalized cloud of sub-micrometric particulates with sizes in the range of 50–400 nm. Some damage to the quartz substrate surface is also observed in the figure. On FTO, similar deposition morphology is observed with larger particulates featuring diameters of 100–400 nm. Damage to the surface of the acceptor material is also observed.

The obtained results clearly show that the laser wavelength has a strong effect on the characteristics of the printed structures. LIFT can be considered as an ablation process under confined geometry [18]. Thus, the lower transfer threshold energy for the shorter wavelength of 248 nm can be related with the different order of the multiphoton process [33]. The photon excitation energy at 248 nm is sufficient to promote the electron to the conduction band of the TiO_2, while two photons are required at 800 nm. Wavelength plays also an important role in the crystallinity of the printed LIFT material. Using wavelengths shorter than the corresponding to the bandgap preserves the crystallinity of the donor, whereas crystallinity is lost at wavelengths larger than that of the bandgap. The tendency of producing smaller nanoparticles at shorter wavelengths, as observed herein, has also been reported in previous studies of fs PLD of TiO_2 [33].

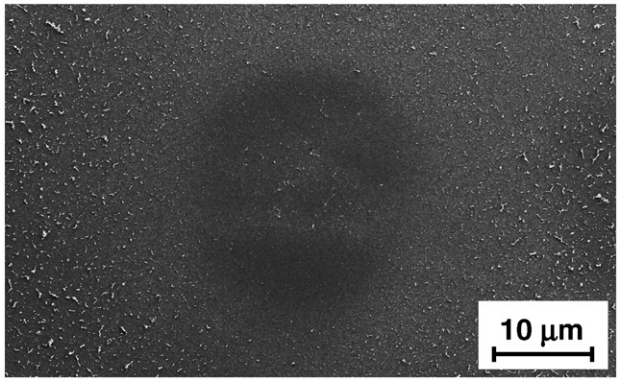

Fig. 5. SEM image of an individual spot of TiO_2 obtained by LIFT at 800 nm on quartz.

4. Conclusions

In conclusion, nanostructured deposits of TiO_2 were prepared on quartz and FTO coated glass substrates by fs LIFT at 248 and 800 nm and were characterized by EDX, XRD, micro-Raman spectroscopy, SEM and AFM. At 248 nm, the material transferred on quartz consists of an underlying irregular layer, about 20 nm thick, covered by round particulates with sizes in the range of 20–200 nm. On FTO, the layer thickness increase to about 35 nm, the concentration of particulates is higher and their size is larger (40–350 nm) due to the fact that these substrates present a rough surface at the nanometer scale that acts as a field of nucleation centres for rutile TiO_2. Rutile polycrystalline deposits were obtained in both types of substrates, with their crystallinity depending on pulse energy. On FTO, the deposits are more crystalline due to the small lattice mismatch which favours the nucleation and growth of rutile crystalline nanoparticles. To obtain a well defined pattern of transferred spots, low energies (2 nJ) are preferred, as using higher pulse energy (22 nJ) results in a larger amount of delocalized material. At 800 nm the deposits are spatially delocalized and not crystalline. At this wavelength, the lowest pulse energy, ensuring material transfer, causes damage to the acceptor material. These results indicate the importance of wavelength and substrate composition in fs LIFT and provide important clues about the processes of laser material printing of customer defined patterns. They also show the possibility of obtaining microstructured arrays of transparent materials without using an absorbing sacrificial layer.

Further work is in progress to improve the morphology and spatial distribution of deposits. More uniform energy distribution in the laser beam, operation in vacuum and optimization of the donor–acceptor distance are foreseen to yield more uniform transfers. Another factor that will be explored is the implementation of temporal shaping of laser pulses to further control the morphology of the transferred features. Finally the fabricated TiO_2 rutile arrays will be tested as substrates for DSSC devices and comparison with an anatase TiO_2 based device will be performed.

Acknowledgements

Funding from MEC, Spain (CTQ2007-60177) and CAM (Geomateriales S2009/MAT 1629) are gratefully acknowledged. This work was carried out at the Ultraviolet Laser Facility operating at IESL-FORTH with support from the access activities of the EC FP7-Infrastructures-2007 project “Laserlab-Europe II” (Grant Agreement No: 212025). M.W. thanks EU (MESTCT-2004-513915) for contract. We are grateful to D. Gómez (Instituto de Ciencia y Tecnología de Polímeros, CSIC) for operating the SEM and Dr. E. Rebollar for AFM measurements.

References

[1] J. Bohandy, B.F. Kim, F.J. Adrian, J. Appl. Phys. 60 (1986) 1538.
[2] J. Bohandy, B.F. Kim, F.J. Adrian, A.N. Jette, J. Appl. Phys. 63 (1988) 1158.
[3] E. Fogarassy, C. Fuchs, F. Kerherve, S. Hauchecorne, J. Perriere, J. Appl. Phys. 66 (1989) 457.
[4] I. Zergioti, S. Mailis, N.A. Vainos, P. Papakonstantinou, C. Kalpouzos, C.P. Grigoropoulos, C. Fotakis, Appl. Phys. A 66 (1998) 579.
[5] P. Papakonstantinou, N.A. Vainos, C. Fotakis, Appl. Surf. Sci. 151 (1999) 159.

[6] I. Zergioti, D.G. Papazoglou, A. Karaiskou, N.A. Vainos, C. Fotakis, Appl. Surf. Sci. 197–198 (2002) 868.
[7] F. Claeyssens, A. Klini, A. Mourka, C. Fotakis, Thin Solid Films 515 (2007) 8529.
[8] Y. Nakata, T. Okada, M. Maeda, Proc. SPIE 3933 (2000) 457.
[9] S. Chakraborty, H. Sakata, E. Yokoyama, M. Wakaki, D. Chakravorty, Appl. Surf. Sci. 254 (2007) 638.
[10] H. Sakata, S. Chakraborty, E. Yokoyama, M. Wakaki, D. Chakravorty, Appl. Phys. Lett. 86 (2005) 114104.
[11] D.P. Banks, K. Kaur, R.W. Eason, Appl. Opt. 48 (2009) 2058.
[12] A. Pique, D. Chrisey, R. Auyeung, J. Fitz-Gerald, H. Wu, R. McGill, S. Lakeou, P. Wu, V. Nguyen, M. Duignan, Appl. Phys. A 69 (1999) S279.
[13] H. Kim, G.P. Kushto, C.B. Arnold, Z.H. Kafafi, A. Piqué, Appl. Phys. Lett. 85 (2004) 464.
[14] H. Kim, R.C.Y. Auyeung, M. Ollinger, G.P. Kushto, Z.H. Kafafi, A. Piqué, Appl. Phys. A 83 (2006) 73.
[15] S. Bera, A.J. Sabbah, J.M. Yarbrough, C.G. Allen, B. Winters, C.G. Durfee, J.A. Squier, Appl. Opt. 46 (2007) 4650.
[16] D.A. Willis, V. Grosu, Appl. Phys. Lett. 86 (2005) 244103.
[17] D.P. Banks, C. Grivas, J.D. Mills, R.W. Eason, I. Zergoiti, Appl. Phys. Lett. 89 (2006) 193107.
[18] A. Klini, P.A. Loukakos, D. Gray, A. Manousaki, C. Fotakis, Opt. Express 16 (2008) 11300.
[19] B. Thomas, A.P. Allonde, P. Delaporte, M. Sentis, S. Sanaur, M. Barret, P. Collot, Appl. Surf. Sci. 254 (2007) 1206.
[20] R. Fardel, M. Nagel, F. Nuesch, T. Lippert, A. Wokaun, Appl. Phys. Lett. 91 (2007) 061103.
[21] D. Banks, K. Kaur, R. Gazia, R. Fardel, M. Nagel, T. Lippert, R. Eason, Europhys. Lett. 83 (2008) 38003.
[22] T. Smausz, B. Hopp, G. Kecskemeti, Z. Bor, Appl. Surf. Sci. 252 (2006) 4738.
[23] E.W. McFarland, J. Tang, Nature 421 (2003) 616.
[24] X. Chen, S.S. Mao, Chem. Rev. 107 (2007) 2891.
[25] M. Grätzel, Nature 414 (2001) 338.
[26] R. Asahi, T. Morikawa, T. Ohwaki, K. Aoki, Y. Taga, Science 293 (2001) 269.
[27] B. Liu, E.S. Aydil, J. Am. Chem. Soc. 131 (2009) 3985.
[28] M. Walczak, E.L. Papadopoulou, M. Sanz, A. Manousaki, J.F. Marco, M. Castillejo, Appl. Surf. Sci. 255 (2009) 5267.
[29] A. Felske, W.J. Plieth, Electrochim. Acta 34 (1989) 75.
[30] Y. Han, G. Wu, M. Wang, H. Chen, Nanotechnology 20 (2009) 235605.
[31] S. Yamamoto, T. Sumita, A. Sugiharuto, A. Miyashita, H. Naramoto, Thin Solid Films 401 (2001) 88.
[32] E. Leveugle, D.S. Ivanov, L.V. Zighlei, Appl. Phys. A 79 (2004) 1643.
[33] M. Sanz, M. Walczak, R. de Nalda, M. Oujja, J.F. Marco, J. Rodríguez, J.G. Izquierdo, L. Bañares, M. Castillejo, Appl. Surf. Sci. 255 (2009) 5206.